Progress in Fractional Differentiation and Applications
An International Journal

http://dx.doi.org/10.18576/pfda/120106

Control and Stability Assessment of a Fractal-Fractional Order Finance System

Muhammad Farman[1,2,3*], *Abdul Sattar Ghaffari*[4], *David Amilo*[1], *Zubaria Parvez*[5], *Aseel Smerat*[6,7], *and Mohamed Hafez*[8,9]

[1] Department of Mathematics, Mathematics Research Center, Near East University, Nicosia /Mersin 10 Turkey
[2] Department of Computer Engineering, Biruni University, Istanbul, Turkey
[3] Research Center of Applied Mathematics, Khazar University, Baku, Azerbaijan
[4] Department of ORIC, Shifa Tameer-e-Millat University, Islamabad, Pakistan
[5] Department of Business Administration, Near East University, Turkey
[6] Faculty of Educational Sciences, Al-Ahliyya Amman University, Amman 19328, Jordan
[7] Department of Biosciences, Saveetha School of Engineering, Saveetha Institute of Medical and Technical Sciences, Chennai, 602105, India
[8] Faculty of Engineering and Quantity Surviving, INTI International University Colleges, Nilai, Malaysia
[9] Faculty of Management, Shinawatra, Pathum Thani, Thailand

Received: 2 Sep. 2025, Revised: 18 Oct. 2025, Accepted: 20 Nov. 2025
Published online: 1 Jan. 2026

Abstract: A novel differential operator is presented that combines fractional and fractal differentiation with a number of different kernels. The connection between fractional calculus and fractals is well-known in the literature, and fractal economic processes are thought to offer more realistic models for economic and financial market issues than traditional models. In order to create a mathematical model for a chaotic financial system that incorporates price measure, investment demands, and minimum rate of interest characteristics, a novel chaotic finance system with a minimal interest rate is built utilizing an extended Mittag-Leffler kernel. We analyze the suggested model using fundamental equations, fixed point notions, and local and global stability. With an emphasis on fractional-order systems, Chaos Control is utilized to control linear reactions. In order to guarantee stability and influence at equilibrium points, the controlled design makes sure that solutions are limited within the possible domain and have an influence at lower minimum interest rates. Using Newton's polynomial-based algorithm, several scenarios are conducted to explore the implications of fractional order and fractal dimension. The results, which were compared using various kernels, are shown by the proportion of minimum interest rates in various countries. In tackling financial and economic growth policy, the results of this study are noteworthy and innovative.

Keywords: Financial development; Fractal fractional model; Qualitative study; Chaos control; Stability analysis.

1 Introduction

The literature on finance, economy, and mathematics frequently addresses macroeconomic inquiry, demand and demand elasticity, and saving and investing rates. Investments and savings are influenced by different factors; investments are more dependent on risk and economic viability, while savings are largely determined by financial status and earnings. These elements are essential to comprehending finance and the economy [1]. Even though they are the results of distinct choices, saving and investing must be treated equally in a closed economy. Time-series and cross-sectional analyses show strong relationships between saving and investment rates, which are lower in smaller economies but greater in large and small ones [2,3]. By sending capital to places with high returns, savings can improve a nations' foreign policy, according to the capital mobility theory. This is especially true for small, open developing nations. When evaluating how foreign direct investment affects domestic capital formation and growth, care should be used [4]. Contrary to conventional macroeconomic theory, which holds that investment limits output growth according to the savings rate, an

* Corresponding author e-mail: farmanlink@gmail.com

increase in national savings will have a greater impact on surplus current account balances and lowering the deficit than it will on local consumption or output growth. According to two articles [5,6], the balance between supply and demand for capital determines the amount of investment in a particular case, with savings presumed to automatically support investments. Even while savings may contribute to the erratic character of demand [7], Domar's examination of the growth model [8] indicates that higher investment is required to sustain full employment. Feldstein and Stock's empirical evidence [9], which demonstrated that investors choose maintaining their savings locally to shield themselves from currency and risk related to politics, reinforced the research' focus on increasing savings and investment rates. Obsefeld's study [10], which is backed by studies in [11,12,13,14], indicates that regional investment and national savings retention are possible even in an extensive open economy like the US. Demand elasticity allows for more accurate understanding of demand fluctuations by measuring how consumers respond to changes in the market [15]. It illustrates how sensitive demand is to shifts in income and price, which are impacted by a number of variables, including cost, revenue, good quality, and customer preferences. The financial sector is shifting towards sustainability and social justice, owing to technical advancements and increased awareness of environmental and societal challenges [16,17].

A mathematical subject that dates back 300 years, fractional calculus is renowned for its memory and capacity to characterize the inherited qualities of materials and processes. It is essential for resolving real-world issues and has attracted the attention of mathematicians, physicists, and engineers in the last ten years [18]-[24]. Since fractional models have been shown to accurately depict a wide range of biological and physical systems and processes, they are a vital tool in many different fields [25]-[30]. The dynamics of a fractional-order delayed zooplankton-phytoplankton system are examined in the paper [31]. It is found that delay has a considerable impact on the stability and Hopf bifurcation time in both fractional-order controlled and fractional-order delayed systems. study [32], which also evaluated the iterative approximate technique using the Adams-Bashforth predictor-corrector scheme. The fractional HBV transmission model was thoroughly examined through the use of computational and mathematical methods. Using an isobutane graph with the chemical formula C_4H_{10} and CAS number 75-28-5, Turab et al. [33] enhanced the mechanism of chemical graph theory. On such graphs, they looked into the existence of solutions to fractional boundary value issues of Caputo type using results from fixed point theory. In his fractional-order financial system [34], Wei-Ching Chen examines chaotic motions, periodical motions, and dynamic behaviors. The lowest order that produces chaos is 2.35, indicating that chaos occurs in systems with orders smaller than 3. The report also pinpoints interruption and period duplication as paths to chaos. [35] discusses a delayed fractional order financial system that is investigated via numerical simulations. It demonstrates that the development of chaos can be either accelerated or inhibited by an approximate time delay, and that the lowest orders of chaos occur at varying delay values. With negative parameters, Tacha et al. [36] created a fractional-order finance system that permitted fractional orders as low as 1.74. By altering the system's eigenvalues, asymptotic stability theorems can be satisfied. For the examination of complex dynamic conduct, nonlinear analysis methods were employed. Wang et al. [37] investigated the dynamics and complexity of a time-delayed fractional-order financial system, noting significant complexity and transitions to deterministic chaos, particularly in reaction to changes in derivative orders. Using terminal sliding mode control and a deep learning recurrent neural network, a novel finite-time technique for regulating and synchronizing fractional-order systems was created [38]. When the method was used on a chaotic financial model, it showed promise in high disturbances. The paper [39] presented a profit-margin hyperchaotic financial system and discussed how to solve it with a fractional-order hyperchaotic finance system based on Caputo derivatives. Recently proposed mathematical tools for handling complicated patterns [40]-[44] are fractal-fractional operators. Because of their complexity, they are helpful for investigating chaotic systems with different dimensions since they generalize fractional and classical operators. Using the fractal-fractional derivative of the Caputo sense, researchers have created a new technique for examining the dynamics of a three-agent financial bubble ([45]). Transition effects were observed in the attractors derived by K. B. Kachhia [46], who used fractal-fractional derivative operators to examine chaos in financial models. For financial marketing, the study in [47] developed a generalized Black-Scholes equation in fractal dimensions, with an emphasis on pricing boundary possibilities and calculating the values of fractal dimensions in time as well as space.

The goal of the work is to develop a new financial model for complex nonlinear differential equations using the fractal-fractional derivative. It analyzes the behavior of financial markets using fractional parameters and the fractional fractal Mittag-Leffler derivative. The fractal-fractional framework aids understanding of financial instability by simulating non-linear, complicated, and memory-dependent market characteristics including volatility clustering and heavy-tailed distributions. Standard models overlook these non-local, scale-invariant fractal dimensions and persistent memory effects, which are critical for effectively forecasting and controlling financial instability during crises. The strong memory effect is better described by the model, which expands upon the fractional order finance model. Additionally, we will go over the characteristics of these operators and show how methods such as the Newton polynomial may be used to quantitatively approximate them.

1.1 Key Definitions

Definition 1.1. [44] On (a,b), let us assume that $\mathbb{M}(t)$ is a fractal differentiable function with order φ. Let $0 \leq \alpha, \varphi \leq 1$, then

– For a power law kernel, we have

$$ {}_0^{FFP}D_t^{\alpha,\varphi}\mathbb{M}(t) = \frac{1}{\Gamma(1-\alpha)}\frac{d}{dt^{\varphi}}\int_0^t (t-\gamma)^{-\alpha}\mathbb{M}(\gamma)d\gamma, \tag{1} $$

where

$$ \frac{d\mathbb{M}(\gamma)}{d\gamma^{\varphi}} = \lim_{t\to\gamma}\frac{\mathbb{M}(t)-\mathbb{M}(\gamma)}{t^{\varphi}-\gamma^{\varphi}}. \tag{2} $$

The integral is defined as

$$ {}_0^{FFP}I^{\alpha,\varphi}\mathbb{M}(t) = \frac{1}{\Gamma(\alpha)}\int_0^t (t-\gamma)^{\alpha-1}\gamma^{1-\varphi}\mathbb{M}(\gamma)d\gamma. \tag{3} $$

– For an exponential decay kernel, we have

$$ {}_0^{FFE}D_t^{\alpha,\varphi}\mathbb{M}(t) = \frac{W(\alpha)}{\Gamma(1-\alpha)}\frac{d}{dt^{\varphi}}\int_0^t \exp\Big[-\frac{\alpha}{1-\alpha}(t-\gamma)\Big]\mathbb{M}(\gamma)d\gamma, \tag{4} $$

where $H(\alpha)$ is normalization function and $W(0) = 1 = W(1)$. The integral is given by

$$ {}_0^{FFE}I^{\alpha,\varphi}\mathbb{M}(t) = \frac{(1-\alpha)t^{1-\varphi}\mathbb{M}(t)}{W(\alpha)} + \frac{\alpha}{W(\alpha)}\int_0^t \gamma^{1-\varphi}\mathbb{M}(\gamma)d\gamma. \tag{5} $$

– For a Mittag-Leffler kernel, we find

$$ {}_0^{FFM}D_t^{\alpha,\varphi}\mathbb{M}(t) = \frac{\text{AB}(\alpha)}{1-\alpha}\frac{d}{dt^{\varphi}}\int_0^t \mathbb{M}(\gamma)\text{E}_{\alpha}\Big[-\frac{\alpha}{1-\alpha}(t-\gamma)^{\alpha}\Big]d\gamma, \tag{6} $$

with $\text{AB}(\alpha) = 1-\alpha+\frac{\alpha}{\Gamma(\alpha)}$ be a normalization function. The integral is

$$ {}_0^{FFM}I^{\alpha,\varphi}\mathbb{M}(t) = \frac{(1-\alpha)t^{1-\varphi}\mathbb{M}(t)}{\text{AB}(\alpha)} + \frac{\alpha}{\text{AB}(\alpha)\Gamma(\alpha)}\int_0^t (t-\gamma)^{\alpha-1}\gamma^{1-\varphi}\mathbb{M}(\gamma)d\gamma. \tag{7} $$

2 Proposed Financial Model

Using the dynamic financial model presented in [48], the objective is to improve the outcomes by adding novel ideas regarding effect interest rate and a practical perspective. Three state variables' time-variation is described in the model as

1. **x**: Interest Rate ,
2. **y**: Investment Demand ,
3. **z**: Price index .

For formulation of model, the following key assumptions are taken into account:

– Two primary causes impact interest rate changes: structural modification from advantageous rates and investment sector incompatibilities or gap between investment and savings.
– The investment demand rate fluctuates with respect to the investment rate and inversion rate, whereas the interest rates and costs of investment have a corresponding impact on the variation in investment demand.
– In commercial markets, the disagreement between supply and demand controls fluctuations in Z, whereas inflation rates also have an impact.
– To understand its effect on investment demand, the study proposes to incorporate the minimal interest rate (κ) into the interest rate (**x**). In order to understand the dynamics of investment, the method uses the interest-investment product to calculate the investment rate (**y**).
– Different countries have different minimum interest rates (κ) to regulate economic conditions. [51] lists interest rates for a number of countries as of August and September 2023, reflecting borrowing and savings returns in each country. For more than a century, real interest rates on safe investments have stayed steady at about 2%, but during the last three decades, they have drastically decreased because of the need for accessibility and security, the slowing expansion of the world economy, and the increased demand for safe assets. Interest rates have stayed historically low despite the global financial crisis; studies conducted in seven different nations since 1870 have shown that safe real interest rates have been declining since about 1980.

By choosing the right coordinate structure and dimensions for state variables, new financial systems can be created using the fractal fractional order derivative as follows:

$$\begin{cases} {}^{FFM}\mathrm{D}_{0,t}^{\alpha,\varphi}(\mathbf{x}(t)) = \mathbf{z} + (\mathbf{y} - \omega)\mathbf{x} + \kappa, \\ {}^{FFM}\mathrm{D}_{0,t}^{\alpha,\varphi}(\mathbf{y}(t)) = 1 - \mathbf{x}^2 - (\eta + \mathbf{x})\mathbf{y}, \\ {}^{FFM}\mathrm{D}_{0,t}^{\alpha,\varphi}(\mathbf{z}(t)) = \kappa - \mathbf{x} - \delta\mathbf{z}, \end{cases} \tag{8}$$

with the initial conditions

$$\mathbf{x}(0) = \mathbf{x}_0 \geq 0, \;\; \mathbf{y}(0) = \mathbf{y}_0 \geq 0, \;\; \mathbf{z}(0) = \mathbf{z}_0 \geq 0, \tag{9}$$

where $\alpha, \varphi \in (0,1]$. In commercial marketplaces, ω, η, and δ stand for the savings, the investment cost, and the demand elasticity, respectively. The non-negative nature of these parameters is evident. Fractal fractional-order finance model (8) provides a complete framework for understanding the intricate, non-local, and memory-specific dynamics of the financial sector. They account for both fractional order (memory effects) and fractal dimension (geographical diversity), yielding greater insights into market behavior and stability than models that just include one feature.

3 Fractional order System's Analysis

3.1 Positive Solutions

Theorem 3.1. If $\mathbf{x}_n(0) \geq 0, \mathbf{y}_n(0) \geq 0, \mathbf{z}_n(0) \geq 0$, $n \in \mathbb{N}$, and $(\mathbf{x}_n, \mathbf{y}_n, \mathbf{z}_n)$ is a solution with any positive beginning conditions concerning the system (8). Then, for all $t \geq 0$, it has $\mathbf{x}_n(t) \geq 0$, $\mathbf{y}_n(t) \geq 0$, $\mathbf{z}_n(t) \geq 0$.

Proof. Consider the norm as

$$||\nu||_\infty = \sup_{t \in D_\nu} |\nu(t)|. \tag{10}$$

We have

$$\begin{aligned} {}^{FFM}\mathrm{D}_{0,t}^{\alpha,\varphi}\mathbf{x}(t) &= \mathbf{z} - (\mathbf{y} - \omega)\mathbf{x} + \kappa, \\ &\geq -(|Y| - \omega)\mathbf{x}, \\ &\geq -(\sup_{t \in D_\mathbf{y}} |\mathbf{y}| - \omega)\mathbf{x} \;=\; -(||\mathbf{y}||_\infty - \omega)\mathbf{x}. \end{aligned} \tag{11}$$

Then, $\forall t \geq 0$, we have [?]:

$$\mathbf{x}(t) \geq \mathbf{x}_0 \; \mathrm{E}_\alpha[-\frac{\upsilon^{1-\varphi}\alpha((||\mathbf{y}||_\infty - \omega)t^\alpha}{\tilde{AB}(\alpha) - (1-\alpha)((||\mathbf{y}||_\infty - \omega)}]. \tag{12}$$

Also, we have

$$\begin{aligned} {}^{FFM}\mathrm{D}_{0,t}^{\alpha,\varphi}(\mathbf{y}(t)) &= 1 - \mathbf{x}^2 - (\eta + \mathbf{x})\mathbf{y}, \\ &\geq -(\eta + |\mathbf{x}|)\mathbf{y}, \\ &\geq -(\eta + \sup_{t \in D_\mathbf{x}} |\mathbf{x}|)\mathbf{x} \;=\; -(\eta + ||\mathbf{x}||_\infty)\mathbf{y}, \end{aligned} \tag{13}$$

so that

$$\mathbf{y}(t) \geq \mathbf{y}_0 \; \mathrm{E}_\alpha[-\frac{\upsilon^{1-\varphi}\alpha((||\mathbf{x}||_\infty + \eta)t^\alpha}{\tilde{AB}(\alpha) - (1-\alpha)((||\mathbf{x}||_\infty + \eta)}], \quad \forall t \geq 0. \tag{14}$$

For the third equation of the system (8), we obtain

$$\mathbf{z}(t) \geq \mathbf{z}_0 \; \mathrm{E}_\alpha[-\frac{\upsilon^{1-\varphi}\alpha(\delta)t^\alpha}{\tilde{AB}(\alpha) - (1-\alpha)(\delta)}]. \tag{15}$$

Theorem 3.2. In addition to starting conditions, the fractional order finance system is distinct and restricted in $\mathbb{R}^3_+$.

Proof: We prove the uniqueness of system over the interval $(0,\infty)$. Thus, it is essential to demonstrate the non-negative region $(\mathbb{R}^3_+)$'s positively invariance. We have

$$^{FFM}\mathrm{D}_{0,t}^{\alpha,\varphi}\mathbf{x}(t)|_{\mathbf{x}=0,\mathbf{z}\geq 0} = \mathbf{z}+\kappa \geq 0, \tag{16}$$
$$^{FFM}\mathrm{D}_{0,t}^{\alpha,\varphi}\mathbf{y}(t)|_{\mathbf{y}=0,\mathbf{x}\geq 0} = 1-\mathbf{x}^2 \geq 0, \tag{17}$$
$$^{FFM}\mathrm{D}_{0,t}^{\alpha,\varphi}\mathbf{z}(t)|_{\mathbf{z}=0,\mathbf{x}\geq 0} = \kappa-\mathbf{x} \geq 0. \tag{18}$$

If $(\mathbf{x}_0,\mathbf{y}_0,\mathbf{z}_0)\in\mathbb{R}^3_+$, then (16) suggests that the hyperplane is an impassable barrier for the solution demonstrating that the domain $\mathbb{R}^3_+$ is positive invariant set. Hence, we conclude that

$$\zeta = \{(\mathbf{x}(t),\mathbf{y}(t),\mathbf{z}(t))\in\mathbb{R}^3_+\}, \tag{19}$$

is the positively invariant region.

3.2 System Solutions' Existence and Uniqueness

The linear growth and Lipschitz conditions, along with fixed-point theorems such as the Banach fixed-point theorem, are used to demonstrate the existence and uniqueness of solutions for fractional-order systems (e.g., [49,50]). The linear growth requirement forbids endlessly massive solutions, whereas the Lipschitz condition ensures that only minor changes in beginning circumstances occur for modest changes, demonstrating uniqueness. These conditions aid in determining solutions within a specified interval. We consider here the system of equations proving the existence and uniqueness of fractional calculus, which requires the following theorem to be proved.

Theorem 3.3. Let the positive constants, ρ_i, $\tilde{\rho}_i$, exist such that

$$a. \quad |\Delta_i^*(\varpi_i,t)-\Delta_i^*(\varpi_i^*,t)|^2 \leq \rho_i|\varpi_i-\varpi_i^*|^2 \quad \forall i,\ i=1,2,3. \tag{20}$$
$$b. \quad |\Delta_i^*(\varpi_i,t)|^2 \leq \tilde{\rho}_i(1+|x_i|) \quad for\ all\ (x,t)\in\mathbb{R}^3\times[0,\mathbf{T}]. \tag{21}$$

Proof. Let

$$\begin{cases} ^{FFM}\mathrm{D}_{0,t}^{\alpha,\varphi}(\mathbf{x}(t)) = \mathbf{z}+(\mathbf{y}-\omega)\mathbf{x}+\kappa &= \Delta_1^*(t,\mathbf{x},\mathbf{y},\mathbf{z}),\\ ^{FFM}\mathrm{D}_{0,t}^{\alpha,\varphi}(\mathbf{y}(t)) = 1-\mathbf{x}^2-(\eta+\mathbf{x})\mathbf{y} &= \Delta_2^*(t,\mathbf{x},\mathbf{y},\mathbf{z}),\\ ^{FFM}\mathrm{D}_{0,t}^{\alpha,\varphi}(\mathbf{z}(t)) = \kappa-\mathbf{x}-\delta\mathbf{z} &= \Delta_3^*(t,\mathbf{x},\mathbf{y},\mathbf{z}). \end{cases} \tag{22}$$

For this reason, we will show that

$$\begin{aligned} |\Delta_1^*(t,\mathbf{x},\mathbf{y},\mathbf{z})-\Delta_1^*(t,\tilde{\mathbf{x}},\tilde{\mathbf{y}},\tilde{\mathbf{z}})|^2 &= |(\mathbf{y}-\omega)(\mathbf{x}-\tilde{\mathbf{x}})|\\ &= \left[2|\mathbf{y}|^2+2\omega^2\right]|\mathbf{x}-\tilde{\mathbf{x}}|^2\\ &= \left[2\sup_{0\leq t\leq \mathbf{T}}|\mathbf{y}|^2+2\omega^2\right]|\mathbf{x}-\tilde{\mathbf{x}}|^2\\ &= \left[2\|\mathbf{y}\|_\infty^2+2\omega^2\right]|\mathbf{x}-\tilde{\mathbf{x}}|^2\\ &\leq \rho_1|(\mathbf{x}-\tilde{\mathbf{x}})|^2, \end{aligned} \tag{23}$$

where $\rho_1 = 2\|\mathbf{y}\|_\infty^2+2\omega^2$.

$$\begin{aligned} |\Delta_2^*(t,\mathbf{x},\mathbf{y},\mathbf{z})-\Delta_2^*(t,\tilde{\mathbf{x}},\tilde{\mathbf{y}},\tilde{\mathbf{z}})|^2 &= |(\eta+\mathbf{x})(\mathbf{y}-\tilde{\mathbf{y}})|\\ &= \left[2\eta^2+|\mathbf{x}|^2\right]|\mathbf{y}-\tilde{\mathbf{y}}|^2\\ &= \left[2\eta^2+2\sup_{0\leq t\leq \mathbf{T}}|\mathbf{x}|^2\right]|\mathbf{y}-\tilde{\mathbf{y}}|^2\\ &= \left[2\eta^2+\|\mathbf{x}\|_\infty^2\right]|\mathbf{y}-\tilde{\mathbf{y}}|^2\\ &\leq \rho_2|(\mathbf{y}-\tilde{\mathbf{y}})|^2, \end{aligned} \tag{24}$$

where $\rho_2 = 2\eta^2 + \|\mathbf{y}\|_\infty^2$.

$$
\begin{aligned}
|\Delta_3^*(t,\mathbf{x},\mathbf{y},\mathbf{z}) - \Delta_3^*(t,\tilde{\mathbf{x}},\tilde{\mathbf{y}},\tilde{\mathbf{z}})|^2 &= |(\delta)(\mathbf{y}-\tilde{\mathbf{y}})| \\
&= \left[2\delta^2\right] |\mathbf{y}-\tilde{\mathbf{y}}|^2 \\
&\leq \rho_3 \left|(\mathbf{y}-\tilde{\mathbf{y}})\right|^2,
\end{aligned} \tag{25}
$$

where $\rho_3 = 2\delta^2$. After that, we obtain

$$
\begin{aligned}
|\Delta_1^*(t,\mathbf{x},\mathbf{y},\mathbf{z})|^2 &= |\mathbf{z} + (\mathbf{y}-\omega)\mathbf{x} + \kappa|^2 \\
&\leq 2|\mathbf{z}|^2 + 2\kappa^2 + 2\left[|\mathbf{y}| - \omega\right]^2 |\mathbf{x}|^2 \\
&\leq 2\left(\sup_{0\leq t\leq \mathbf{T}} |\mathbf{z}|^2 + \kappa^2\right) + 2\left[\sup_{0\leq t\leq \mathbf{T}} |\mathbf{y}| - \omega\right]^2 |\mathbf{x}|^2 \\
&\leq 2\left(\|\mathbf{z}\|_\infty^2 + \kappa^2\right) + 2\left[\|\mathbf{y}\|_\infty - \omega\right]^2 |\mathbf{x}|^2 \\
&\leq 2\left(\|\mathbf{z}\|_\infty^2 + \kappa^2\right)\left\{1 + \frac{\|\mathbf{y}\|_\infty - \omega}{\|\mathbf{z}\|_\infty^2 + \kappa^2} |\mathbf{x}|^2\right\} \\
&\leq \tilde{\rho}_1 \left(1 + |\mathbf{x}|^2\right),
\end{aligned} \tag{26}
$$

under the condition $\frac{\|\mathrm{y}\|_\infty - \omega}{\|\mathbf{z}\|_\infty^2 + \kappa^2} < 1$.

$$
\begin{aligned}
|\Delta_2^*(t,\mathbf{x},\mathbf{y},\mathbf{z})|^2 &= \left|1 - \mathbf{x}^2 - (\eta + \mathbf{x})\mathbf{y}\right|^2 \\
&\leq 2 + 2\left|\mathbf{x}^2\right|^2 + 2\left[\eta + |\mathbf{x}|\right]^2 |\mathbf{y}|^2 \\
&\leq 2\left(1 + \sup_{0\leq t\leq \mathbf{T}} |\mathbf{x}^2|^2\right) + 2\left[\eta + \sup_{0\leq t\leq \mathbf{T}} |\mathrm{x}|\right]^2 |\mathbf{y}|^2 \\
&\leq 2\left(1 + \|\mathbf{x}^2\|_\infty^2\right) + 2\left[\eta + \|\mathbf{x}\|_\infty\right]^2 |\mathbf{y}|^2 \\
&\leq 2\left(1 + \|\mathbf{x}^2\|_\infty^2\right)\left\{1 + \frac{\eta + \|\mathbf{x}\|_\infty}{1 + \|\mathbf{x}^2\|_\infty^2} |\mathbf{y}|^2\right\} \\
&\leq \tilde{\rho}_2 \left(1 + |\mathbf{y}|^2\right),
\end{aligned} \tag{27}
$$

under the condition $\frac{\eta + \|\mathbf{x}\|_\infty}{1 + \|\mathbf{x}^2\|_\infty^2} < 1$.

$$
\begin{aligned}
|\Delta_3^*(t,\mathbf{x},\mathbf{y},\mathbf{z})|^2 &= |\kappa - \mathbf{x} - \delta\mathbf{z}|^2 \\
&\leq 2\kappa^2 + 2|\mathbf{x}|^2 + 2\delta^2 |\mathbf{z}|^2 \\
&\leq 2\left(\kappa^2 + \sup_{0\leq t\leq \mathbf{T}} |\mathbf{x}|^2\right) + 2\delta^2 |\mathbf{z}|^2 \\
&\leq 2\left(\kappa^2 + \|\mathbf{x}\|_\infty^2\right) + 2\delta^2 |\mathbf{z}|^2 \\
&\leq 2\left(\kappa^2 + \|\mathbf{x}\|_\infty^2\right)\left\{1 + \frac{\delta^2}{\kappa^2 + \|\mathbf{x}\|_\infty^2} |\mathbf{z}|^2\right\} \\
&\leq \tilde{\rho}_3 \left(1 + |\mathbf{z}|^2\right),
\end{aligned} \tag{28}
$$

under the condition $\frac{\delta^2}{\kappa^2 + \|\mathbf{x}\|_\infty^2} < 1$.
Because of this, our system has a unique answer for the following situations.

$$
\max \begin{cases} \frac{\|\mathrm{y}\|_\infty - \omega}{\|\mathbf{z}\|_\infty^2 + \kappa^2} \\ \frac{\eta + \|\mathbf{x}\|_\infty}{1 + \|\mathbf{x}^2\|_\infty^2} \\ \frac{\delta^2}{\kappa^2 + \|\mathbf{x}\|_\infty^2} \end{cases} < 1. \tag{29}
$$

To demonstrate uniqueness in contraction mappings, these coefficients must be less than or equal to one. They must meet the Lipschitz condition, which ensures that each iteration of a function goes closer to a unique fixed point, ”shrinking” the interval holding the solution and preventing numerous distinct solutions from coexisting.

3.3 Equilibrium Points

All of the system (8)'s equations can be equated to zero in order to identify the system's equilibrium points by determining the point of engagement at the zero-growing isoclines.

$$\begin{aligned} \mathbf{z} + (\mathbf{y} - \omega)\mathbf{x} + \kappa &= 0, \\ 1 - \mathbf{x}^2 - (\eta + \mathbf{x})\mathbf{y} &= 0, \\ \kappa - \mathbf{x} - \delta \mathbf{z} &= 0. \end{aligned} \tag{30}$$

The following equilibrium points result from selecting $\omega = 3$, $\eta = 0.1$, and $\delta = 1$ as the parameters:

$$\begin{aligned} &P_1(\mathbf{x},\ \mathbf{y},\ \mathbf{z}) = (0.6449,\ 0.8785,\ 0.3676), \\ &P_2(\mathbf{x},\ \mathbf{y},\ \mathbf{z}) = (0.586,\ 0.8305,\ 0.3633), \\ &P_3(\mathbf{x},\ \mathbf{y},\ \mathbf{z}) = (0.6213,\ 0.886,\ 0.349). \end{aligned} \tag{31}$$

4 Stability and Chaos Control

With an emphasis on the stability features of the selected model, this part employs a number of theorems to illustrate the local and global stability as well as the chaos management of fractional order financial systems.

4.1 Local Asymptotical Stability

Theorem 4.1. When the reproductive number is less than 1, our system (8)'s equilibrium point, P_1, is locally asymptotically stable in the feasible region.

Proof. System (8)'s Jacobian matrix evaluated at equilibrium point is provided by

$$\mathbb{J}(P^*) = \begin{bmatrix} \mathbf{y} - \omega & \mathbf{x} & 1 \\ -2\mathbf{x} - \mathbf{y} & -\mathbf{x} - \eta & 0 \\ -1 & 0 & -\delta \end{bmatrix}. \tag{32}$$

One way to express the characteristic equation is as follows:

$$f(\psi) = \begin{vmatrix} \psi - \mathbf{y} + \omega & -\mathbf{x} & -1 \\ 2\mathbf{x} + \mathbf{y} & \psi + \eta + \mathbf{x} & 0 \\ 1 & 0 & \psi + \delta \end{vmatrix} \tag{33}$$

$$\begin{aligned} &= \psi^3 + \psi^2(\mathbf{x} + \eta + p + \omega - \mathbf{y}) + \psi(\eta\delta + (\omega - \mathbf{y})(\eta + \delta + \mathbf{x}) + \mathbf{x}(\delta + 2\mathbf{x} + \mathbf{y}) + 1) \\ &+ (\eta + \mathbf{x})(\omega\delta - \mathbf{y}\delta + 1) + \mathbf{x}\mathbf{y}(2\mathbf{x} + \delta). \end{aligned} \tag{34}$$

At P_1 and the parameters $\omega = 3$, $\eta = 0.1$, $\delta = 1$, we get

$$f(\psi) = \psi^3 + 3.8664\psi^2 + 6.8450\psi + 3.6224 = 0, \tag{35}$$

and the corresponding eigenvalues are

$$\psi_1 = -1.5116 + 1.4180\imath, \quad \psi_2 = -1.5116 - 1.4180\imath, \quad \psi_3 = -0.8433. \tag{36}$$

Therefore, P_1 is locally asymptotically stable in the feasible region.

4.2 Global Stability Analysis

Theorem 4.2. When the reproductive number exceeds 1, our system (8)'s equilibrium points are globally asymptotically stable.

Proof. Let the Lyapunov function is as follows:

$$\mathbb{M} = \rho_1(\mathbf{x}-\mathbf{x}^*-\mathbf{x}^*\ln\frac{\mathbf{x}}{\mathbf{x}^*})+\rho_2(\mathbf{y}-\mathbf{y}^*-\mathbf{y}^*\ln\frac{\mathbf{y}}{\mathbf{y}^*})+\rho_3(\mathbf{z}-\mathbf{z}^*-\mathbf{z}^*\ln\frac{\mathbf{z}}{\mathbf{z}^*}), \tag{37}$$

Following from Lemma [?], we get

$$^{FFM}\mathrm{D}_{0,t}^{\alpha,\varphi}\mathbb{M} \le \rho_1(1-\frac{\mathbf{x}^*}{\mathbf{x}})^{FFM}\mathrm{D}_{0,t}^{\alpha,\varphi}\mathbf{x}+\rho_2(1-\frac{\mathbf{y}^*}{\mathbf{y}})^{FFM}\mathrm{D}_{0,t}^{\alpha,\varphi}\mathbf{y}+\rho_3(1-\frac{\mathbf{z}^*}{\mathbf{z}})^{FFM}\mathrm{D}_{0,t}^{\alpha,\varphi}\mathbf{z}. \tag{38}$$

Substituting derivatives' values

$$\begin{aligned} ^{FFM}\mathrm{D}_{t}^{\alpha,\varphi}\mathbb{M} \le{}& \rho_1(1-\frac{\mathbf{x}^*}{\mathbf{x}})\left[\mathbf{z}+(\mathbf{y}-\omega)\mathbf{x}+\kappa\right]+\rho_2(1-\frac{\mathbf{y}^*}{\mathbf{y}})\left[1-\mathbf{x}^2-(\mathbf{x}+\eta)\mathbf{y}\right] \\ &+\rho_3(1-\frac{\mathbf{z}^*}{\mathbf{z}})(\kappa-\mathbf{x}-\delta\mathbf{z}). \end{aligned} \tag{39}$$

We assume that $\mathbf{x}=\mathbf{x}-\mathbf{x}^*$, $\mathbf{y}=\mathbf{y}-\mathbf{y}^*$, and $\mathbf{z}=\mathbf{z}-\mathbf{z}^*$, then we get

$$\begin{aligned} ^{FFM}\mathrm{D}_{t}^{\alpha,\varphi}\mathbb{M} \le{}& \rho_1(1-\frac{\mathbf{x}^*}{\mathbf{x}})\left[(\mathbf{z}-\mathbf{z}^*)+((\mathbf{y}-\mathbf{y}^*)-\omega)(\mathbf{x}-\mathbf{x}^*)+\kappa\right] \\ &+\rho_2(1-\frac{\mathbf{y}^*}{\mathbf{y}})\left[1-(\mathbf{x}-\mathbf{x}^*)^2-((\mathbf{x}-\mathbf{x}^*)+\eta)(\mathbf{y}-\mathbf{y}^*)\right] \\ &+\rho_3(1-\frac{\mathbf{z}^*}{\mathbf{z}})\left[\kappa-(\mathbf{x}-\mathbf{x}^*)-\delta(\mathbf{z}-\mathbf{z}^*)\right]. \end{aligned} \tag{40}$$

We have

$$\begin{aligned} ^{FFM}\mathrm{D}_{t}^{\alpha,\varphi}\mathbb{M} \le{}& \mathbf{z}-\mathbf{z}^*\frac{\mathbf{x}^*}{\mathbf{x}}+(\mathbf{y}-\mathbf{y}^*)\frac{(\mathbf{x}-\mathbf{x}^*)^2}{\mathbf{x}}-\omega\frac{(\mathbf{x}-\mathbf{x}^*)^2}{\mathbf{x}}-\kappa\frac{\mathbf{x}^*}{\mathbf{x}}+1-\frac{\mathbf{y}^*}{\mathbf{y}} \\ &-(\mathbf{x}-\mathbf{x}^*)^2+(\mathbf{x}-\mathbf{x}^*)^2\frac{\mathbf{y}^*}{\mathbf{y}}-(\mathbf{x}-\mathbf{x}^*)\frac{(\mathbf{y}-\mathbf{y}^*)^2}{\mathbf{y}}-\eta\frac{(\mathbf{y}-\mathbf{y}^*)^2}{\mathbf{y}} \\ &+2\kappa-\kappa\frac{\mathbf{z}^*}{\mathbf{z}}-(\mathbf{x}-\mathbf{x}^*)+(\mathbf{x}-\mathbf{x}^*)\frac{\mathbf{z}^*}{\mathbf{z}}-\delta\frac{(\mathbf{z}-\mathbf{z}^*)^2}{\mathbf{z}}. \end{aligned} \tag{41}$$

Let $\rho_1=1$, $\rho_2=1$, and $\rho_3=1$, then we have

$$^{FFM}\mathrm{D}_{0,t}^{\alpha,\varphi}\mathbb{M} = U_1-U_2, \tag{42}$$

where

$$U_1 = \mathbf{z}+(\mathbf{y}-\mathbf{y}^*)\frac{(\mathbf{x}-\mathbf{x}^*)^2}{\mathbf{x}}+1+(\mathbf{x}-\mathbf{x}^*)^2\frac{\mathbf{y}^*}{\mathbf{y}}+2\kappa+(\mathbf{x}-\mathbf{x}^*)\frac{\mathbf{z}^*}{\mathbf{z}}, \tag{43}$$

and

$$\begin{aligned} U_2 ={}& \mathbf{z}^*\frac{\mathbf{x}^*}{\mathbf{x}}+\omega\frac{(\mathbf{x}-\mathbf{x}^*)^2}{\mathbf{x}}+\kappa\frac{\mathbf{x}^*}{\mathbf{x}}-\frac{\mathbf{y}^*}{\mathbf{y}}+(\mathbf{x}-\mathbf{x}^*)^2+(\mathbf{x}-\mathbf{x}^*)\frac{(\mathbf{y}-\mathbf{y}^*)^2}{\mathbf{y}}+\eta\frac{(\mathbf{y}-\mathbf{y}^*)^2}{\mathbf{y}} \\ &+\kappa\frac{\mathbf{z}^*}{\mathbf{z}}+(\mathbf{x}-\mathbf{x}^*)+\delta\frac{(\mathbf{z}-\mathbf{z}^*)^2}{\mathbf{z}}. \end{aligned} \tag{44}$$

$^{FFM}\mathrm{D}_{0,t}^{\alpha,\varphi}\mathbb{M}=0$ if and only if $x=x^*$, $y=y^*$, and $z=z^*$, and $^{FFM}\mathrm{D}_{0,t}^{\alpha,\varphi}\mathbb{M}<0$ if $U_1<U_2$, have been noted. A reproductive number bigger than one, however, results in equilibrium P^*, and the singleton set $\{P^*\}$ is the greatest compact invariant set in

$$\{(\mathbf{x},\ \mathbf{y},\ \mathbf{z})\in\zeta\ :\ ^{FFM}\mathrm{D}_{0,t}^{\alpha,\varphi}\mathbb{M}=0\}. \tag{45}$$

The equilibrium points are therefore globally asymptotically stable in ζ if $U_1<U_2$ according to Lasalle's invariance principle.

4.3 Chaos Control

Linear feedback can be used to regulate fractal fractional order finance models, thereby stabilizing chaotic markets and attaining market synchrony. This methodology governs factors such as interest rates, stock prices, and foreign exchange rates, offering a straightforward, low-cost, and easy-to-implement strategy for managing financial volatility and creating more stable, predictable, and harmonious market circumstances. While state input controllers use eigenvalues and Jacobian system matrices to stabilize fractional chaotic systems, we will employ the linear feedback regulate technique, which uses equilibrium points to stabilize system (8). By introducing three control parameters; ϕ_1, ϕ_2, and ϕ_3, we get

$$\begin{cases} {}^{FFM}\mathrm{D}_{0,t}^{\alpha,\varphi}(\mathbf{x}(t)) = \mathbf{z}+\mathbf{xy}-\omega\mathbf{x}+\kappa-\phi_1(\mathbf{x}-\mathbf{x}^*), \\ {}^{FFM}\mathrm{D}_{0,t}^{\alpha,\varphi}(\mathbf{y}(t)) = 1-\eta\mathbf{y}-\mathbf{x}^2-\mathbf{xy}-\phi_2(\mathbf{y}-\mathbf{y}^*), \\ {}^{FFM}\mathrm{D}_{0,t}^{\alpha,\varphi}(\mathbf{z}(t)) = \kappa-\mathbf{x}-\delta\mathbf{z}-\phi_3(\mathbf{z}-\mathbf{z}^*), \end{cases} \tag{46}$$

System (8)'s Jacobian matrix determined at equilibrium point is given by

$$\mathbb{J}(P^*) = \begin{bmatrix} \mathbf{y}-\omega-\phi_1 & \mathbf{x} & 1 \\ -2\mathbf{x}-\mathbf{y} & -\mathbf{x}-\eta-\phi_2 & 0 \\ -1 & 0 & -\delta-\phi_3 \end{bmatrix}. \tag{47}$$

The characteristic equation can be expressed in the following way:

$$f(\vartheta) = \begin{vmatrix} \vartheta-\mathbf{y}+\omega+\phi_1 & -\mathbf{x} & -1 \\ 2\mathbf{x}+\mathbf{y} & \vartheta+\eta+\mathbf{x}+\phi_2 & 0 \\ 1 & 0 & \vartheta+\delta+\phi_3 \end{vmatrix} = 0. \tag{48}$$

Let $\phi_1 = 1$ $\phi_2 = 2$ and $\phi_3 = 3$. If $\omega = 3$, $\eta = 0.1$, $\delta = 1$. Therefore,

– At P_1, we have

$$f(\vartheta) = \vartheta^3 + 9.8664\vartheta^2 + 37.1321\vartheta + 50.7110 = 0, \tag{49}$$

and we get

$$\vartheta_1 = -3.3170 + 2.1647\imath, \quad \vartheta_2 = -3.3170 - 2.1647\imath,$$
$$\vartheta_3 = -3.2324.$$

– At P_2, we have

$$f(\vartheta) = \vartheta^3 + 9.8555\vartheta^2 + 36.808742\vartheta + 49.5329 = 0, \tag{50}$$

and

$$\vartheta_1 = -3.3393 + 2.1073\imath, \quad \vartheta_2 = -3.33393 - 2.1073\imath,$$
$$\vartheta_3 = -3.1770.$$

– At P_3, we have

$$C(\vartheta) = \vartheta^3 + 9.8353\vartheta^2 + 36.8378\vartheta + 50.00780 = 0, \tag{51}$$

and

$$\vartheta_1 = -3.3098 + 2.1439\imath, \quad \vartheta_2 = -3.3098 - 2.1439\imath,$$
$$\vartheta_3 = -3.2157.$$

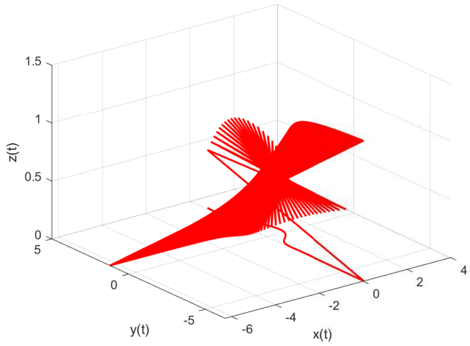

Fig. 1: **xyz** at $\varphi = 0.01$

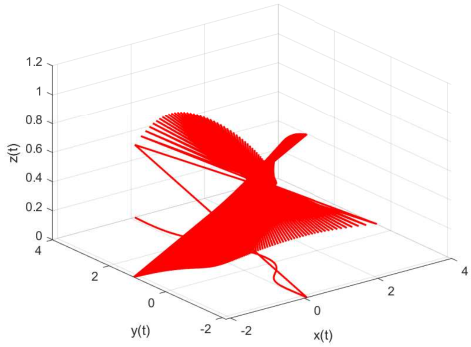

Fig. 2: **xyz** at $\varphi = 0.01$

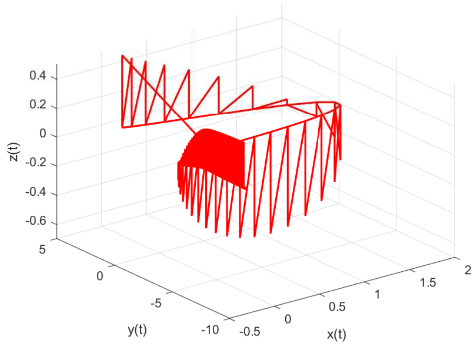

Fig. 3: **xyz** at $\kappa = 1$

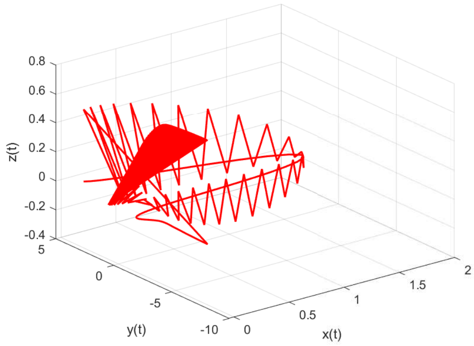

Fig. 4: **xyz** at $\kappa = 5$

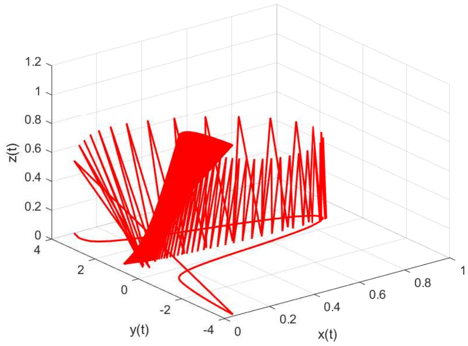

Fig. 5: $\kappa = 2.5$, $\varphi = 0.1$

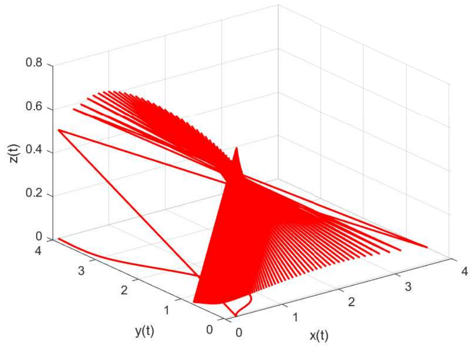

Fig. 6: $\kappa = 2.5$, $\varphi = 0.6$

Fig. 7: Proposed system's chaotic behaviour

Equations (50), (51), and (52) all have eigenvalues that are either negative real numbers or complex numbers with a negative real component. As a result, the system (8)'s are asymptotically stable for every $0 < \kappa < 5$. The simulation of the designed system, as depicted in Figure (7), demonstrates that solutions have a greater influence at lower minimum interest rates and are bounded in the feasible region. The suggested model's chaos can be further controlled using a variety of strategies, including nonlinear feedback controls, sliding type control, passive control, adaptive control, delayed response control, and active control. These techniques seek to turn chaotic financial systems into organized states, with advantages in speed, robustness, and complexity over linear approaches.

5 Numerical Method

A numerical algorithm for the numerical results of a new finance system employing the generalized version of the fractal-fractional derivative with an initial condition is presented in this section. A helpful technique for fractal-fractional system solving is the Newton polynomial, which provides better management of non-linear and chaotic dynamics, a simpler mathematical representation, and increased accuracy through the addition of more data points. When analytical methods are not practical, this method offers an accurate and effective numerical solution to complicated problems. The steps of the proposed approach are described in pseudocode by the following.

– Consider the problem

$$\begin{aligned} {}^{FFM}\mathrm{D}_{0,t}^{\alpha,\varphi}\bar{\chi}(t) &= \lambda(t,\bar{\chi}(t)), \quad t\in[0,\mathbf{T}], \\ \bar{\chi}(0) &= \bar{\chi}_0, \end{aligned} \tag{52}$$

where $\lambda(t,\bar{\chi}(t))$ denotes a nonlinear function.

– Let h be the step size for temporal discretization and T be the total simulation duration. The number of steps is calculated using

$$N=\frac{T}{h},$$

and

$$t_k = kh, \qquad k=0,1,2,...,N.$$

Note: For the solution of the proposed model, we set $h=0.2$, $T=200$, and number of iterations=1000.

– Rewrite the equation (52) by means of the fractional integral utilizing definitions.

– Discrete the integral using Newton polynomial interpolation.

– To estimate $\delta(t,\mathrm{G}(t))$ over the interval $[t_k,t_{k+1}]$, apply a two-step Newton polynomial. Substitute it into the integral to perform a quantitative calculation.

– Determine the numerical scheme of G_{k+1}.

– G_0 should be the initial condition. G_{k+1} for $N=0,1,2,...,N-1$ should be calculated.

Suppose that

$$\begin{cases} {}^{FFM}\mathrm{D}_{0,t}^{\alpha,\varphi}(\mathbf{x}(t)) = \xi_1(t,\mathbf{x},\mathbf{y},\mathbf{z}), \\ {}^{FFM}\mathrm{D}_{0,t}^{\alpha,\varphi}(\mathbf{y}(t)) = \xi_2(t,\mathbf{x},\mathbf{y},\mathbf{z}), \\ {}^{FFM}\mathrm{D}_{0,t}^{\alpha,\varphi}(\mathbf{z}(t)) = \xi_3(t,\mathbf{x},\mathbf{y},\mathbf{z}). \end{cases} \tag{53}$$

Now, let the Cauchy problem be as given in (52) where $\bar{\chi}=\{\mathbf{x},\mathbf{y},\mathbf{z}\}$. Once the integral has been used, the Volterra formula is given by

$$\bar{\chi}\left(t_{\varsigma+1}\right) = C_{1_0} + \frac{1-\alpha}{\text{A̧B}(\alpha)} t_\varsigma^{1-\varphi}\lambda\left(t_\varsigma,\bar{\chi}\left(t_\varsigma\right)\right) + \text{A̧B}\sum_{r=2}^{\varsigma}\int_{t_0}^{t_0+1}\lambda\left(\gamma,\bar{\chi}(\gamma)\right)\gamma^{1-\varphi}\left(t_{\varsigma+1}-\gamma\right)^{\alpha-1}d\gamma. \tag{54}$$

Utilizing Newton polynomial, we get

$$\begin{aligned} \bar{\chi}\left(t_{\varsigma+1}\right) = \bar{\chi}_0 &+ \frac{1-\alpha}{\text{A̧B}(\alpha)} t_\varsigma^{1-\varphi}\lambda\left(\mathrm{t}_\varsigma,\bar{\chi}(t_\varsigma)\right) + \frac{\alpha}{\text{A̧B}(\alpha)\Gamma(\alpha)}\left[\sum_{r=2}^{\varsigma}\lambda\left(\mathrm{t}_\varsigma,\bar{\chi}(t_\varsigma)\right)t_{\varsigma-2}^{1-\varphi}\int_{t_0}^{t_0+1}\left(t_{\varsigma+1}-\gamma\right)^{\alpha-1}d\gamma\right. \\ &+\sum_{r=2}^{\varsigma}\frac{1}{\Delta t}\left\{t_{\varsigma-1}^{1-\varphi}\lambda[\mathrm{t}_{\varsigma-1},\bar{\chi}^{\varsigma-1}(t)] - t_{\varsigma-1}^{1-\varphi}\lambda[\mathrm{t}_{\varsigma-2},\bar{\chi}^{\varsigma-2}(t)]\right\}\int_{t_0}^{t_0+1}\left(\gamma-t_{\varsigma-2}\right)\left(t_{\varsigma+1}-\gamma\right)^{\alpha-1}d\gamma \\ &+\sum_{r=2}^{\varsigma}\frac{1}{\Delta t^2}\left\{t_0^{1-\varphi}\lambda[\mathrm{t}_r,\bar{\chi}^r(t)] - 2t_{\varsigma-1}^{1-\varphi}\lambda[\mathrm{t}_{\varsigma-1},\bar{\chi}^{\varsigma-1}(t)] + t_{\varsigma-2}^{1-\varphi}\lambda[\mathrm{t}_{\varsigma-2},\bar{\chi}^{\varsigma-2}(t)]\right\} \\ &\left.\times\int_{t_0}^{t_0+1}\left(\gamma-t_{\varsigma-2}\right)\left(\gamma-t_{\varsigma-1}\right)\left(t_{\varsigma+1}-\gamma\right)^{\alpha-1}d\gamma\right]. \end{aligned} \tag{55}$$

Following several computations, we ultimately obtain

$$
\begin{aligned}
\bar{\chi}(\mathrm{t}_{\varsigma+1}) = {} & \bar{\chi}_0 + \frac{1-\alpha}{\mathrm{AB}(\alpha)}\mathrm{t}_{\varsigma}^{1-\varphi}\lambda[\mathrm{t}_{\varsigma},\bar{\chi}(t_{\varsigma})] + \frac{\alpha(\Delta \mathrm{t})^{\alpha}}{\mathrm{AB}(\alpha)\Gamma(\alpha+1)}\sum_{r=2}^{\varsigma}\lambda[\mathrm{t}_{\varsigma},\bar{\chi}(t_{\varsigma})]\mathrm{t}_{\mathrm{r}-2}^{1-\varphi}[(1+\varsigma-r)^{\alpha}-(\varsigma-r)^{\alpha}] \\
& + \frac{\alpha(\Delta \mathrm{t})^{\alpha}}{\mathrm{AB}(\alpha)\Gamma(\alpha+2)}\sum_{r=2}^{\varsigma}\frac{1}{\Delta \mathrm{t}}\left\{\mathrm{t}_{r-1}^{1-\varphi}\lambda\left[\mathrm{t}_{\varsigma-1},\bar{\chi}^{\varsigma-1}(t)\right] - \mathrm{t}_{r-2}^{1-\varphi}\lambda\left[\mathrm{t}_{\varsigma-2},\bar{\chi}^{\varsigma-2}(t)\right]\right\} \\
& \qquad \times[(1+\varsigma-r)^{\alpha}(3+2\alpha+\varsigma-r)-(\varsigma-r)^{\alpha}(3(1+\alpha)+\varsigma-r)] \\
& + \frac{\alpha(\Delta \mathrm{t})^{\alpha}}{\mathrm{AB}(\alpha)\Gamma(\alpha+3)}\sum_{r=2}^{\varsigma}\frac{1}{2\Delta \mathrm{t}^2}\left\{\mathrm{t}_{r}^{1-\varphi}\lambda[\mathrm{t}_r,\bar{\chi}^{r}(t)] - 2\mathrm{t}_{r-1}^{1-\beta}\lambda[\mathrm{t}_{\varsigma-1},\bar{\chi}^{\varsigma-1}(t)] + \mathrm{t}_{r-2}^{1-\varphi}\lambda[\mathrm{t}_{\varsigma-2},\bar{\chi}^{\varsigma-2}(t)]\right\} \\
& \times\Big[(1+\varsigma-r)^{\alpha}\{2(\varsigma-r)^2+(3\alpha+10)(\varsigma-r)+(2\alpha+9)\alpha+12\} \\
& \quad -(\mathrm{s}-r)^{\alpha}\{2(\varsigma-r)^2+(5\alpha+10)(\varsigma-r)+6\alpha(\alpha+3)+12\}\Big].
\end{aligned}
\tag{56}
$$

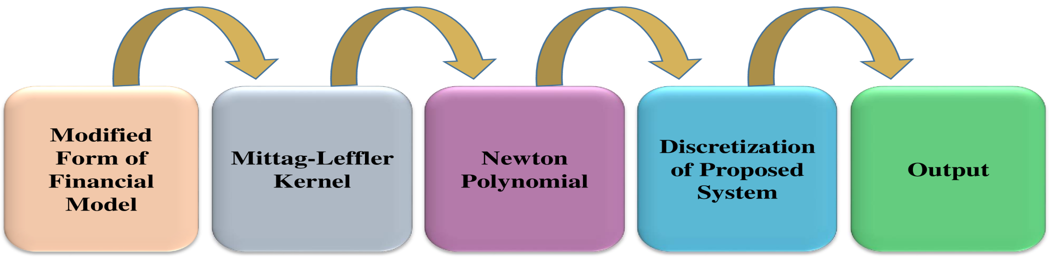

Fig. 8: Bayesian algorithm flowchart of the system

The numerical scheme stability principle states that very few errors in the numerical solution will arise from minor changes to the initial condition. Examine the scheme's solutions, denoted by χ_i for $(i = 1,2,...,k)$. In this case, mathematical induction offers a practical method:

$$
|\chi_i - \overline{\chi}_i| \leq \varpi_{\alpha,\mathbf{T}}\|\chi_0 - \overline{\chi}_0\|_{\infty}, \tag{57}
$$

where $\varpi_{q,\mathbf{T}} > 0$ is a constant. This is still the case for $(i = 0,1,2,...,k)$. The evidence needs to be confirmed for $i = k+1$ in order to be finished. The proof can now be concluded for sufficiently small $\mathbf{T}$ by employing a mathematical induction and a large enough constant $\varpi_{\alpha,\mathbf{T}}$.

6 Result and Discussion

Appropriate analytical solutions for a number of non-integer dynamical systems are absent from numerical solutions. In order to illustrate how fractal-fractional order affects a phenomenon's dynamics, we thus utilized numerical methods based on Newton polynomials to fractal-fractional operators. We used MATLAB software to solve the computational solution.

The outcomes show how fractal-fractional operators affect the dynamical system, especially when complex features are taken into account. Figures are used to display the numerical solution. The initial conditions are:

$$\mathbf{x}_0 = 0.1, \quad \mathbf{y}_0 = 4, \quad \mathbf{z}_0 = 0.5.$$

Better estimation of minimal interest rate values utilizing data [48] from different countries, such as interest rate, investment demand, and price multiplier rate, is made possible by the financial system's fractal fractional derivative. The impact is displayed at various fractal and fractional order values in Figures (12-24), which also demonstrate the accuracy and speed of convergence of the suggested operator in a fractal sense. The proposed financial model, which has the lowest feasible rate of interest, is constructed by adding the parameter κ to this system. As shown in figures (12-24), economic power is increased at the lowest minimum interest rate due to a greater price exponent and a rise in investment needs. To combat the poverty rate in society as a whole increase the origin of income and develop a new financial strategy. Additionally, consider the impact of the shifting dimensions in figures 16 and 24. Under the fractalfractional derivative with different kernels, figures (28-40) are obtained using similar numerical schemes, demonstrating that the choice of α and ϑ values in an economic model with stable equilibrium points is arbitrarily determined, with the goal of achieving stable outcomes for its equilibrium points.

Significant responses are displayed by the model's compartments, where the link between the variables either grows or decreases. Macroeconomic behavior is demonstrated by the rise in interest rates with initial investment consumption and the fall in price variables. In contrast to time-integer factors, complex chaotic fractional systems are more appropriate and reliable for non-integer time-fractional factors, reflecting the true macroeconomic activity of the financial system. According to the findings, fractal fractional analysis is superior at forecasting future economic control and minimizing the gap between financial units. When studying steady states with non-integer-order derivatives, it yields reliable answers for every compartment, and fractional value reduction improves the precision and dependability of solutions. By altering the fractal dimension, memory influence can be shown with a solution limited to a viable steady state point and a higher degree of freedom.

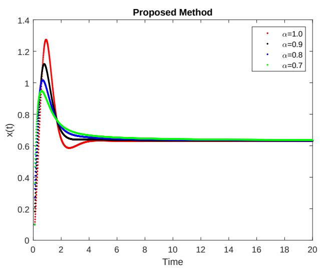

Fig. 9: $\mathbf{x}(t)$

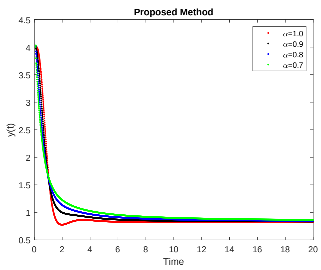

Fig. 10: $\mathbf{y}(t)$

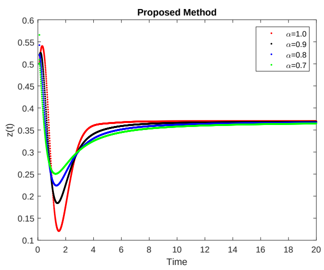

Fig. 11: $\mathbf{z}(t)$

Fig. 12: Proposed system simulation with various α values and $\varphi = 1$ with $\kappa = 1$

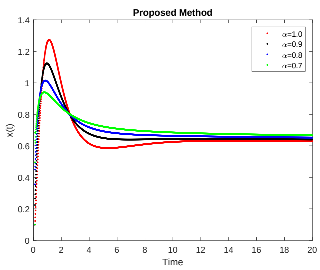

Fig. 13: $\mathbf{x}(t)$

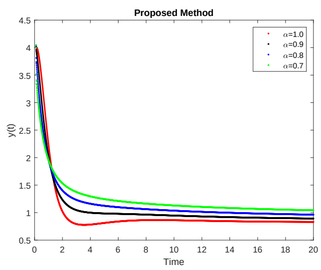

Fig. 14: $\mathbf{y}(t)$

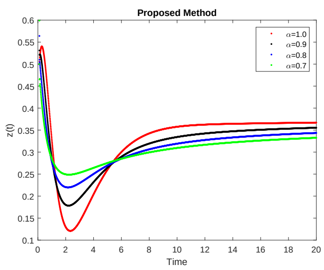

Fig. 15: $\mathbf{z}(t)$

Fig. 16: Proposed system simulation with various α values and $\varphi = 0.6$ with $\kappa = 1$

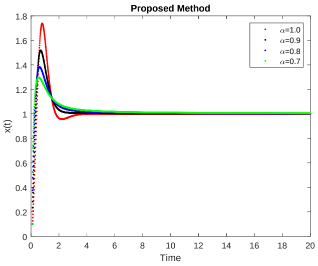

Fig. 17: $\mathbf{x}(t)$

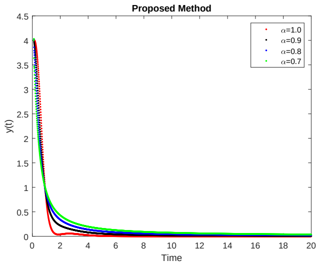

Fig. 18: $\mathbf{y}(t)$

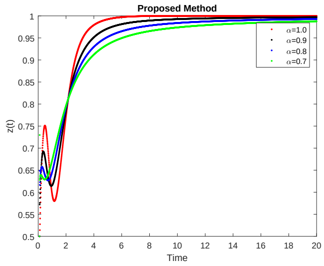

Fig. 19: $\mathbf{z}(t)$

Fig. 20: Proposed system simulation with various α values and $\varphi = 1$ with $\kappa = 2$

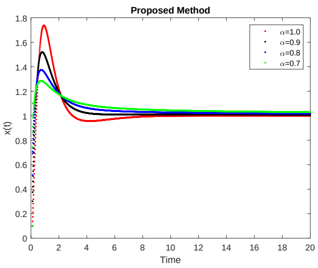

Fig. 21: $\mathbf{x}(t)$

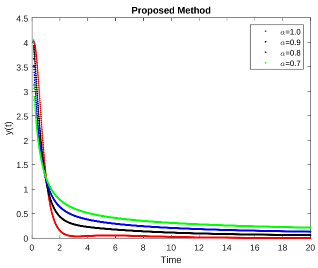

Fig. 22: $\mathbf{y}(t)$

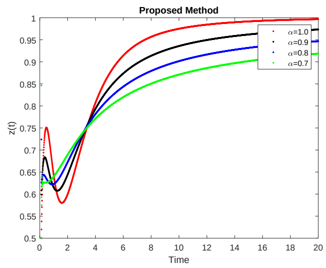

Fig. 23: $\mathbf{z}(t)$

Fig. 24: Proposed system simulation with various α values and $\varphi = 0.6$ with $\kappa = 2$

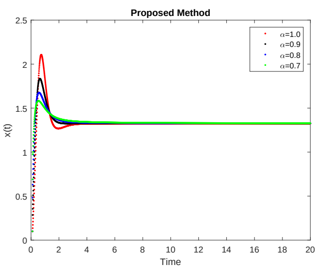

Fig. 25: $\mathbf{x}(t)$

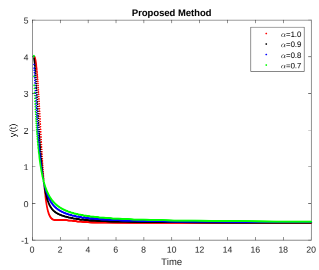

Fig. 26: $\mathbf{y}(t)$

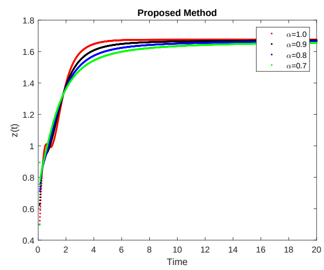

Fig. 27: $\mathbf{z}(t)$

Fig. 28: Proposed system simulation with various α values and $\varphi = 1$ with $\kappa = 3$

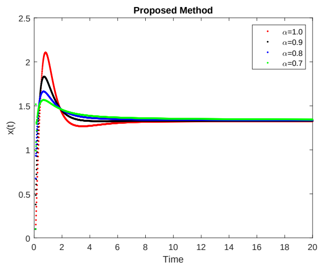

Fig. 29: $\mathbf{x}(t)$

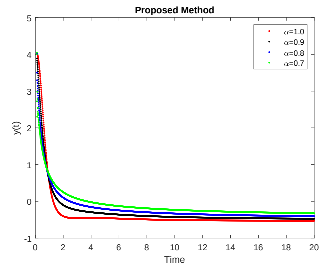

Fig. 30: $\mathbf{y}(t)$

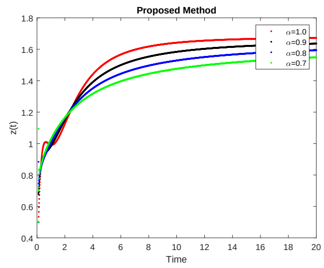

Fig. 31: $\mathbf{z}(t)$

Fig. 32: Proposed system simulation with various α values and $\varphi = 0.6$ with $\kappa = 3$

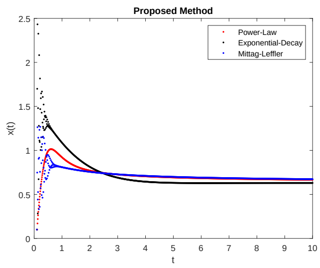

Fig. 33: $\mathbf{x}(t)$

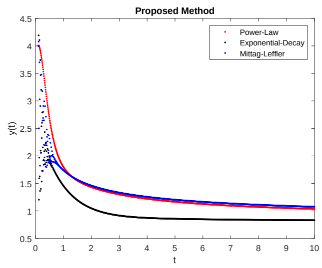

Fig. 34: $\mathbf{y}(t)$

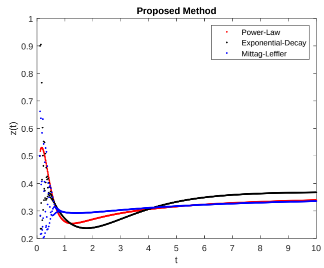

Fig. 35: $\mathbf{z}(t)$

Fig. 36: Proposed system simulation with various kernels at $\alpha = 0.7$

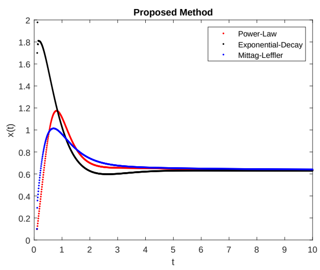

Fig. 37: $\mathbf{x}(t)$

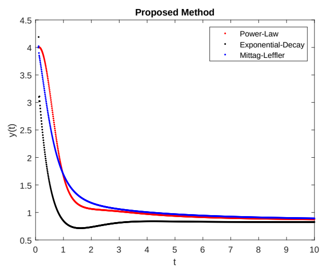

Fig. 38: $\mathbf{y}(t)$

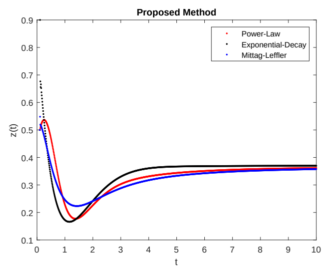

Fig. 39: $\mathbf{z}(t)$

Fig. 40: Proposed system simulation with various kernels at $\alpha = 0.9$

Variations in fractional order (α) in the proposed finance model influence memory effects and convergence rates, with greater values potentially resulting in faster convergence but not stability. While changes in fractal dimension (ϑ) capture the complexity and self-similarity of market activity, they also influence volatility and risk by modeling market behavior patterns. Researchers can utilize variable-order fractional models to represent market memory and combine fractal analysis and fractional calculus to connect market complexity to memory dynamics, thereby boosting risk management and portfolio optimization. Future work can use tables to correlate parameter ranges to macroeconomic outcomes such as volatility or market stability, hence improving interpretation. A sensitivity analysis can also be performed by adjusting the fractal and fractional orders to see how they affect critical variables such as GDP or inflation.

7 Conclusions

A fractal fractional operator comprehension of the Mittag-Leffler function was used in this work to test a novel fractal-fractional financial model both theoretically and numerically. Through local and global stability tests, the model's stability is confirmed, and it guaranteed the uniqueness and positivity of solutions inside the feasible zone. Strong agreement on the financial management of the system was demonstrated by the use of the model to control the economy's fundamentally low interest rate. The percentage of minimum interest rates in different nations was utilized as a stand-in for the results, which were compared using different kernels. A number of scenarios are carried out to investigate the effects of fractal dimension and fractional order. By incorporating memory and heterogeneity, the fractal-fractional operator offered robustness for the study of financial system dynamics. Results indicate that the financial market's complexity is better expressed by the fractal-fractional model. Additionally, convergence shows that the proposed system is stable. Using numerical data, we also examined how the essential minimum interest rate affected price coefficients, interest rates, and investment demand over time. It demonstrates how interest rates increase in accordance with initial conditions when investment demand as well as price exponents decline, exposing the underlying macroeconomic dynamics of the financial system. In order to improve comprehension of financial markets, future research will build on this by examining sophisticated mathematical models, mathematical algorithms, and variable ordering of derivatives, as well as by implementing efficient control mechanisms.

References

[1] A. Chouchane-Verdier, Une analyse empirique de l'impact de la libéralisation financière en Afrique subsaharienne sur la période 1983-1996, *Revue Tiers Monde*, **179**(3), 617-641, (2004).
[2] R. M. Solow, A contribution to the theory of economic growth, *The quarterly journal of economics*, **70**(1), 65-94,(1956).
[3] T. W. Swan, Economic growth and capital accumulation, *Economic record*, **32**(2), 334-361, (1956).
[4] R. E. Lucas Jr, On the mechanics of economic development, *Journal of monetary economics*, **22**(1), 3-42, (1988).
[5] R. R. Palmer, Turgot: paragon of the continental enlightenment, *The Journal of Law and Economics*, **19**(3), 607-619, (1978).
[6] G. J. Benston and C. W. Smith, A transactions cost approach to the theory of financial intermediation, *The Journal of finance*, **31**(2), 215-231, (1976).
[7] J. M. Keynes, The general theory of employment, *The quarterly journal of economics*, **51**(2), 209-223, (1937).
[8] E. D. Domar, Expansion and employment, *The American Economic Review*, **37**(1), 34-55, (1947).
[9] M. Feldstein and J. H. Stock, The use of a monetary aggregate to target nominal GDP. In *Monetary policy* (pp. 7-69), The University of Chicago Press, (1994).
[10] M. Obstfeld, How integrated are world capital markets? Some new tests, (1986).
[11] M. H. Tobin-Ríchards, A. M. Boxer and A. C. Petersen, The psychological significance of pubertal change: Sex differences in perceptions of self during early adolescence, *Girls at puberty: Biological and psychosocial perspectives*, 127-154, (1983).
[12] L. Dramani, *Les déterminants de l'investissement privé au Sénégal: une approche VAR structurel*, Republique du Senegal, Ministere de l'Economie et des Finances, (2008).
[13] L. J. Esso, and Y. Keho, The savings-investment relationship: Cointegration and causality evidence from Uemoa countries, *International Journal of Economics and Finance*, **2**(1), 174-181, (2010).
[14] N. Dries, and R. Pepermans, How to identify leadership potential: Development and testing of a consensus model, *Human Resource Management*, **51**(3), 361-385, (2012).
[15] G. Vaggi, P. Groenewegen, G. Vaggi, and P. Groenewegen, Alfred Marshall, 1842-1924: Partial Equilibrium and Useful Economics, *A Concise History of Economic Thought: From Mercantilism to Monetarism*, 227-234, (2003).
[16] T. L. Le, J. W. Goodell, R. Khalfaoui, E. J. A. Abakah,and B. Dogan, The impact of economic outlook on green finance: insights from linkages between green and inflation-indexed bonds, *Environment, Development and Sustainability*, **27**(3), 6507-6538, (2025).
[17] F. Abuamria and M. Ajouz, Leveraging FinTech Innovations for Sustainable and Social Finance: A Comprehensive Analysis of Their Contributions to Social Impact Investment, In *From Digital Disruption to Dominance (pp. 245-264)*, Emerald Publishing Limited, (2025).
[18] H. Benbouhenni, I. Colak, N. Bizon, and E. Abdelkarim, Fractional-order neural control of a DFIG supplied by a two-level PWM inverter for dual-rotor wind turbine system, *Measurement and Control*, **57**(3), 301-318, (2024).
[19] C. Hu, and Y. Ji, Filtering-based gradient joint identification algorithms for nonlinear fractional-order models with colored noises, *Communications in Nonlinear Science and Numerical Simulation*, **130**, 107759, (2024).
[20] K. S. Nisar, M. O. Kulachi, A. Ahmad, M. Farman, M. Saqib, and M. U. Saleem, Fractional order cancer model infection in human with CD8+ T cells and anti-PD-L1 therapy: simulations and control strategy, *Scientific Reports*, **14**(1), 16257, (2024).
[21] H. Benbouhenni, N. Bizon, M. I. Mosaad, I. Colak, A. B. Djilali, and H. Gasmi, Enhancement of the power quality of DFIG-based dual-rotor wind turbine systems using fractional order fuzzy controller, *Expert Systems with Applications*, **238**, 121695, (2024).

[22] S. Jamil, K. Jamil, and A. Shehzad, Modeling and Stability Analysis of the Unemployment Model with Caputo, *Journal of Mathematical Modeling and Fractional Calculus*, **1**(2), 23-39, (2025).
[23] S. Verma and A. Dwivedi, Integral Transform and Generalized M-Series Fractional Integral Operators, *Journal of Mathematical Modeling and Fractional Calculus*, **2**(1), 1-18, (2025).
[24] P. Yadav, S. Jahan, and K. S. Nisar, Solving fractional Bagley-Torvik equation by fractional order Fibonacci wavelet arising in fluid mechanics. *Ain Shams Engineering Journal*, **15**(1), 102299, (2024).
[25] A. Ahmad, M. Farman, P. A. Naik, K. Faiz, A. Ghaffar, E. Hincal, and M. U. Saleem, Analytical analysis and bifurcation of pine wilt dynamical transmission with host vector and nonlinear incidence using sustainable fractional approach, *Partial Differential Equations in Applied Mathematics*, **11**, 100830, (2024).
[26] S. Momani, R. Sharma, J. Singh, Y. Singh, and S. Hadid, Fractional order mathematical modelling for studying the impact on the emergence of pollution and biodiversity pertaining to incomplete Aleph functions, *Progress in Fractional Differentiation and Applications*, **10**(1), 15-22, (2024).
[27] C. Xu, M. Farman, and A. Shehzad, Analysis and chaotic behavior of a fish farming model with singular and non-singular kernel, *International Journal of Biomathematics*, 2350105, (2023).
[28] X. Kong, F. Yu, W. Yao, S. Cai, J. Zhang, and H. Lin, Memristor-induced hyperchaos, multiscroll and extreme multistability in fractional-order HNN: Image encryption and FPGA implementation, *Neural Networks*, **171**, 85-103, (2024).
[29] K. S. Nisar, M. Farman, E. Hincal, and A. Shehzad, Modelling and analysis of bad impact of smoking in society with Constant Proportional-Caputo Fabrizio operator, *Chaos, Solitons & Fractals*, **172**, 113549, (2023).
[30] C. Xu, M. Liao, M. Farman, and A. Shehzad, Hydrogenolysis of glycerol by heterogeneous catalysis: a fractional order kinetic model with analysis, *MATCH Communications in Mathematical and in Computer Chemistry*, **91**(3), 635-664, (2024).
[31] P. Li, R. Gao, C. Xu, Y. Li, A. Akgül, and D. Baleanu, Dynamics exploration for a fractional-order delayed zooplankton-phytoplankton system, *Chaos, Solitons & Fractals*, **166**, 112975, (2023).
[32] A. Turab, R. Shafqat, S. Muhammad, M. Shuaib, M. F. Khan, and M. Kamal, Predictive modeling of hepatitis B viral dynamics: a caputo derivative-based approach using artificial neural networks. *Scientific Reports*, **14**(1), 21853, (2024).
[33] A. Turab, W. Sintunavarat, and J. S. Ro, On novel mathematical modeling for studying a class of nonlinear Caputo-type fractional-order boundary value problems emerging in CGT. *Fractal and Fractional*, **7**(2), 99, (2023).
[34] W. C. Chen, Nonlinear dynamics and chaos in a fractional-order financial system, *Chaos, Solitons & Fractals*, **36**(5), 1305-1314, (2008).
[35] Z. Wang, X. Huang, and G. Shi, Analysis of nonlinear dynamics and chaos in a fractional order financial system with time delay, *Computers & Mathematics with Applications*, **62**(3), 1531-1539, (2011).
[36] O. I. Tacha, J. M. Munoz-Pacheco, E. Zambrano-Serrano, I. N. Stouboulos, and V. T. Pham, Determining the chaotic behavior in a fractional-order finance system with negative parameters, *Nonlinear Dynamics*, **94**, 1303-1317, (2018).
[37] S. Wang, S. He, A. Yousefpour, H. Jahanshahi, R. Repnik, and M. Perc, Chaos and complexity in a fractional-order financial system with time delays, *Chaos, Solitons & Fractals*, **131**, 109521, (2020).
[38] Y. L. Wang, H. Jahanshahi, S. Bekiros, F. Bezzina, Y. M. Chu, and A. A. Aly, Deep recurrent neural networks with finite-time terminal sliding mode control for a chaotic fractional-order financial system with market confidence, *Chaos, Solitons & Fractals*, **146**, 110881, (2021).
[39] M. D. Johansyah, A. Sambas, S. Qureshi, S. Zheng, T. M. Abed-Elhameed, S. Vaidyanathan, and I. M. Sulaiman, Investigation of the hyperchaos and control in the fractional order financial system with profit margin, *Partial Differential Equations in Applied Mathematics*, **9**, 100612, (2024).
[40] K. A. Abro and A. Atangana, Mathematical modeling of neuron model through fractal-fractional differentiation based on maxwell electromagnetic induction: application to neurodynamics, *Neural Computing and Applications*, **36**(29), 18377-18385, (2024).
[41] M. Farman, A. Akgül, M. S. Hashemi, L. Guran, and A. Bucur, Fractal Fractional Order Operators in Computational Techniques for Mathematical Models in Epidemiology. *CMES-Computer Modeling in Engineering & Sciences*, **138**(2), (2024).
[42] M. Farman, A. Shehzad, K. S. Nisar, E. Hincal, and A. Akgül, A mathematical fractal-fractional model to control tuberculosis prevalence with sensitivity, stability, and simulation under feasible circumstances, *Computers in Biology and Medicine*, **178**, 108756, (2024).
[43] A. Kumar, S. Kumar, S. Momani, and S. Hadid, A chaos study of fractal-fractional predator-prey model of mathematical ecology, *Mathematics and Computers in Simulation*, **225**, 857-888, (2024).
[44] M. Izadi and A. Atangana, Computational analysis of a class of singular nonlinear fractional multi-order heat conduction model of the human head, *Scientific Reports*, **14**(1), 3466, (2024).
[45] B. Li, T. Zhang, and C. Zhang, Investigation of financial bubble mathematical model under fractal-fractional Caputo derivative, *Fractals*, **31**(05), 2350050, (2023).
[46] K. B. Kachhia, Chaos in fractional order financial model with fractal-fractional derivatives, *Partial Differential Equations in Applied Mathematics*, **7**, 100502, (2023).
[47] R. A. El-Nabulsi and W. Anukool, Qualitative financial modelling in fractal dimensions. *Financial Innovation*, **11**(1), 42, (2025).
[48] W. C. Chen, Nonlinear dynamics and chaos in a fractional-order financial system, *Chaos, Solitons & Fractals*, **36**(5), 1305-1314, (2008).

[49] Y. Zhao, C. Xu, Y. Xu, J. Lin, Y. Pang, Z. Liu, and J. Shen, Mathematical exploration on control of bifurcation for a 3D predator-prey model with delay, *AIMS Math*, **9**(11), 29883-29915, (2024).
[50] J. Lin, C. Xu, Y. Xu, Y. Zhao, Y. Pang, Z. Liu and J. Shen, Bifurcation and controller design in a 3D delayed predator-prey model, *AIMS Math*, **9**(12), 33891-33929, (2024).
[51] Trading Economics (2024), Interest Rate - Countries - List, Tradingeconomics.com. https://tradingeconomics.com/country-list/interest-rate